Journal of Chemical Health Risks

www.jchr.org

JCHR (2025) 15(5), 465-493 | ISSN:2251-6727

Exploring Heterocyclic Compounds as Potent Malaria falcipain-2 Inhibitors versus Cathepsins: A Computational Approach

Kavita Sharma[1], Vandana Pandey[1*], Virender[2], Archit Sharma[3], Brij Mohan[4], Neera Raghav[1*]

[1]Department of Chemistry, Kurukshetra University, Kurukshetra-136119, Haryana, India,

[2]Department of Chemistry, Deenbandhu Chhotu Ram University of Science & Technology, Murthal, Sonepat, 131039, Haryana, India

[3]University Institute of Engineering and Technology, Kurukshetra University, Haryana, India

[4]Centro de Química Estrutural, Institute of Molecular Sciences, Instituto Superior Técnico, Universidade de Lisboa, Av. Rovisco Pais, 1049-001 Lisboa, Portugal

(Received: 16 July 2025 Revised: 20 August 2025 Accepted: 02 September 2025)

KEYWORDS

Heterocyclic compounds, antimalarial, drug-likeness, QSAR, molecular modeling, bioactivity score, ADME, toxicity.

ABSTRACT:

Malaria, caused by Plasmodium parasites, leads to 400,000+ annual deaths, primarily affecting women and children in Asia and sub-Saharan Africa. Increasing medication resistance highlights the urgent need for better treatment strategies.

Falcipain-2, a cysteine protease in Plasmodium falciparum, is a crucial drug target but shares similarities with cathepsins, making selectivity essential in antimalarial therapy. Curcumin, a chalcone from turmeric, shows antimalarial properties but has bioavailability issues. This study explores modified curcumin analogs, specifically monocarbonyl curcumins, which lack the retro-aldol breakdown group. Computational approaches, including protein alignment, QSAR modeling, and in-silico techniques, were used to assess their bioavailability, solubility, stability, and toxicity.

QSAR modeling successfully predicted log% inhibitory activities of (E)-chalcones as falcipain-2 inhibitors using a nonlinear (ANN) method. The QSAR model was validated with external compounds, and statistical analysis confirmed its robustness. The GA-ANN model's mean-squared errors (MSEs) were 0.045 for training and 0.063 for test sets. 28 new molecules (D1-D28) were designed and optimized, with predicted log% inhibition values. Docking studies of the most potent analogs (D9 & D10), curcumin, and standard drugs in falcipain-2 and cathepsin were conducted. Analog D9, with an affinity of -10.1 kcal/mol, showed strong selectivity for falcipain-2 over cathepsin. Further analyses evaluated bioavailability, solubility, stability, and toxicity for future in vitro and in vivo studies.

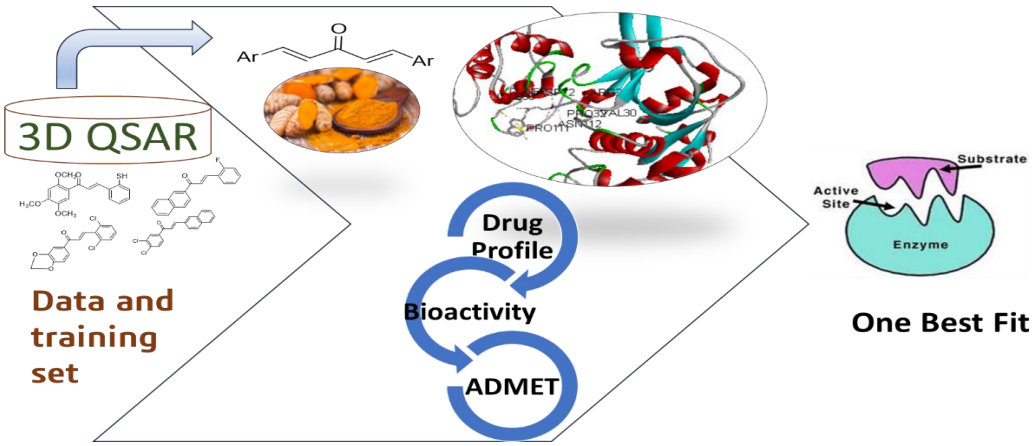

Journal of Chemical Health Risks

www.jchr.org

JCHR (2025) 15(5), 465-493 | ISSN:2251-6727

1. Introduction.

Malaria is a fatal infectious illness caused by Plasmodium parasites spread by mosquitoes [1,2]. It claims over 400,000 lives yearly, primarily affecting children in sub-Saharan Africa [3]. Despite progress, challenges like drug resistance persist, underscoring the urgent need for effective prevention, treatment, and continued research to combat its lethal impact globally. Approximately1.3millionin the form of research grant was used to develop potential anti-malarial drug. Two primary antimalarial drugs, chloroquine and artemether, are now limited by adverse effects, short half-lives, and the need for repeated daily dosages[4]. In several cases alternative treatment or drug is required. The ongoing exploration for novel molecular targets in drug design aims to expand the therapeutic toolkit and enhance strategies against drug resistance in human malaria.

Preliminary drug molecule research and development, safety assessment, benefited significantly to the discovery of possible therapeutic targets. Traditional drug discovery involves time-consuming experimental processes, including screening large chemical libraries, synthesizing and testing compounds, and iteratively optimizing leads for therapeutic efficacy, safety and yet may lead to total darkness in terms of output [5]. However rapid virtual screening reduces the need for synthesizing and testing numerous compounds[6]. Thus in-silico approaches expedite target identification, accelerating anti-malarial drug discovery and saving resources. Especially QSAR (quantitative structure activity relationship) which is a mathematical equation corelating target property with structural feature[7], Docking studies to insight interaction between target protein and our analogs and drug profiling have been extensively used in drug discovery[8].

Falcipains have been described as cysteine proteases expressed in the blood stages of the malaria parasite *Plasmodium falciparum* and participate in the degradation of hemoglobin in the endosomal compartments of the parasite[9,10]. Falcipain-2 an important drug target for antimalarial therapy share structural and functional similarities with cathepsins, particularly cathepsin L-like enzymes[11]. Cathepsins are lysosomal proteases found in various organisms, including humans, and are involved in protein degradation, antigen processing, and other cellular processes [12]. Anticathepsin have been the focus of our research group's effort[13,14] and the homology between falcipain and cathepsin confirmed by us through in-silico protein structure pair alignment, is significant and it allows us to study the anticathepsin against target enzymes in the context of antimalarial drug development[15]. Inhibitors designed against cathepsins have been explored for their potential to inhibit falcipain and disrupt the malaria parasite's lifecycle.

Curcuminis a specific type of chalcone found in turmeric, characterized by its vibrant yellow color is well reported anticathepsin in our lab[16] and also exhibit notable antimalarial efficacy [17,18]. Curcumin **figure I (a)**, though demonstrating promising antimalarial activity in in-vitro and in-vivo studies, faces several limitations. Its poor bioavailability, limited solubility, and rapid metabolism hinder its efficacy[19]. Challenges in specificity, potential

Journal of Chemical Health Risks

www.jchr.org

JCHR (2025) 15(5), 465-493 | ISSN:2251-6727

drug interactions, and insufficient liver stage inhibition contribute to concerns. The risk of resistance development, limited clinical data, and variability in curcumin content across sources further complicate its utilization as a reliable antimalarial drug. An unexplored approach to address the bioavailability challenge of curcumin as an antimalarial agent is structural modification. Designing curcumin analogs resistant to rapid breakdown in blood plasma could be evaluated for potential antimalarial activity through screening processes.Chalcones, in general, are a broader class of natural phenolic compounds featuring two aromatic rings connected by an α,β-unsaturated carbonyl system, present in various plants, sharing a common structural feature with curcumin[20],present a promising avenue for antimalarial activity. Research indicates their potential to inhibit the growth and replication of Plasmodium, the malaria parasite. The structural diversity of chalcones allows for modifications, optimizing pharmacological properties[21].

This study proposes the *in-silico* investigation of monocarbonyl curcumin compounds, synthetic analogs of curcumin **figure I (b)** as inhibitor of Falcipain-2. These curcumins lack the CH_2CO group, which is associated with the retro-aldol breakdown of curcumin in blood plasma[22]. In this work, we performed the QSAR modelling on some set of reported (E) Chalcones with inhibition against Fac-2 and predicted the proposed inhibition activity of some novel designed curcumin analogs using constructed model. Furthermore, interactions of most potent inhibitors with target were analyzed using molecular docking and compared with mammalian cathepsin. Along with great affinity for falcipain-2 their drug profile for better assimilation into body and safety in terms of toxicity was also studied for their emergence as a potent and safe drug.

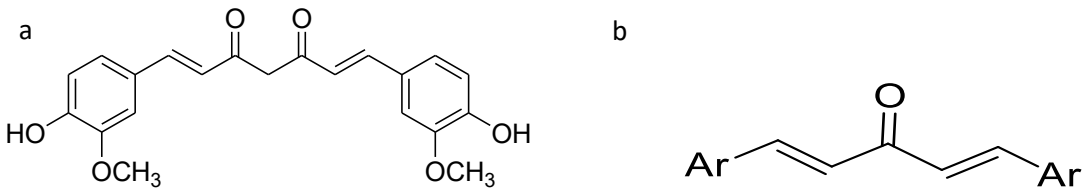

Figure I: a-Structure of curcumin b-Designed compound

2. Method

2.1 Determination of Sequence pair alignment and chemistry of both proteins

In order to check the homology between the cathepsin and falcipain, their sequence data was obtained from Protein Data Bank (PDB) a consolidated database for protein structure determined experimentally by usingtechniques X-ray crystallography or NMR spectroscopy. Sequence pair alignment between cathepsin B, H, L and falcipain-2 were compared using PDB alignment tool and using seeded guide trees and HMM profile-profile approaches, Clustal Omega Server which is a novel multiple sequence alignment application that creates alignments between three or more sequences[23,24]. For better relation between their modes of inhibition and interaction with catalytic triad pocket was studied by prank web server. Itutilizes various algorithms and approaches, such as geometric, energetic, or

Journal of Chemical Health Risks
www.jchr.org
JCHR (2025) 15(5), 465-493 | ISSN:2251-6727

evolutionary considerations, to predict potential binding pockets on protein structures.

2.2 QSAR modelling

The series of 82 chalcones and their log% inhibition activities were taken from the work published by Bertoldo et al[25] . The target activity datset was first converted into logarithmic scale and then values of log% (-0.0644 to 1.4154) were used in QSAR modeling as the response variables. The experimental log% values of the chalcones are presented in the **table I**. The 3d-geometries of the chalcones were optimized using MMFF94 force field and the Steepest Descent Algorithm with 500 steps of minimization. Descriptors were calculated with the Dragon software[26]. Descriptors in various catagories were generated for each compound including like molecular properties, 2D autocorelations, constitutional descriptors, eigenvalue-based indices, topological descriptors, topological charge indices, connectivity indices, information indices, geometrical descriptors, 3D-Morse, walk and path counts, Getaway, WHIM and RDF descriptors. The selection of the optimal subset of descriptors is a crucial step in developing a reliable QSAR model. To obtain the optimal subset for non-linear QSAR mapping, objective and subjective feature selection techniques were used. The well known vWSP algorithm was used to reduce redundancy in the dataset after deleting the constant and near constant variables from the descriptor pool. Then, genetic algorithm (GA) was applied to the reduced pool to search the feature space and descriptors that were pertinent to the inhibitory values were chosen [27]. The following is a list of the important variables that affected the GA performance: total number of iterations=100, mutation probability=0.5, the initial number of equations generated=100, crossover probability=1, Fitness fuction= FF1(based on Error/MAE based parameters) (R). A vital and crucial step in QSAR modelling is the selection of the best data division strategy. For meaningful predictions, the complete dataset with 82 chalcones was divided into training set and test set using Kennard-Stone algorithm. A fully connected, three layered, feed-forward artificial neural network was employed to explore the non-linear relationship between the selected descriptors and inhibitory activity. The ANN's architecture was such that (a) the neurons in the input layer equals the descriptors selected from the GA approach, (b) the number of hidden nodes was optimized, and (c) the output neuron was the target activity for each molecule. Standard numerical optimization algorithm (Levenberg-Marquardt (LM) was used to train the ANNs.

Model validation is a crucial component of QSAR modeling to verify the reliability and robustness of the created QSAR model. The developed GA-ANN QSAR models were validated by external validation method using test set.) Various parameters recommended by Golbraikh and Tropsha as well as mean absolute percent error (mape), root mean squared error (rmse) were calculated for evaluation of prediction capability of proposed models, Thorough inspection of dataset revealed the presence of heterocyclic ring is responsible for improved inhibition activity. On the basis of this, some new heterocyclic compounds were designed and the developed model was used to predict inhibition activity of these newly designed analogues **(table III)**.

Journal of Chemical Health Risks
www.jchr.org
JCHR (2025) 15(5), 465-493 | ISSN:2251-6727

Then the designed analogs and best reference compound (66) were docked against cathepsins and faclcipain-2 for better insight interactions.

2.3 Molecular Docking

Some promisinganalogs were docked into the fal-2 as well as cathepsins to study the molecular basis of interaction and affinity of binding of curcumin and its analogs via AUTODOCK VINA[28] (http://vina.scripps.edu/) based on gradient optimization algorithm and the results were further revalidate by using iGEMDOCK software[29] (http://gemdock.life.nctu.edu.tw/dock/download.php)based on generic evolutionary method (GA). And the results are compared with curcumin, reported reference compound 66 and standard drugs docked into fal-2 andcathepsins under same conditions.

2.3.1 AUTODOCK VINA

3D crystallographic structure of protein was downloaded from Protein data bank (www.pdb.org) with pdb id 2IPP[30], 8PCH[31], 3BC3[32], 3BPF[33] for cathepsin B, H, L, and fac-2 respectivelyand then processed in mgl tools (http://mgltools.sripps.edu/downloads) by adding polar H atoms and removing water molecules to avoid any interference in binding analysis. For good docking analysis quantum mechanically calculated chemical partial charge of each amino acid i.e. Kollmann charges were also added and saved as acceptable pdbqt file format. Additionally, cathepsins were processed in DS visualizer to extract and get a grid box of binding site, and the configuration was based on binding ofthe inhibitor in PDB file of, CathB, CathH, CathL, and fac-2 respectively. The grid box dimension in Armstrong units is (x, y, z) = (-13.7960, 74.346714, -52.490), (6.584282, 24.921094, 29.757087), (-5.930325, 15.954233, 15.805617), (-58.055613 3.013736 -29.714764) and centred at coordinates (x, y, z) = (40, 40, 40) respectively for CathB, CathH, CathL, and fac-2.All the docking was performed with 8 runs for better insight of binding. In addition, the best selected pose was again docked with protein under same configuration [34].

2.3.2 iGEMDOCK

To revalidate Autodock results, ligands were again docked and redocked using iGemdock. For this, appropriate PDB and MOL formats, protein and ligand structure files were generated. It assisted in the specification and preparation of the binding sites. The docking efficiency required the following parameters to be set: There are 300 members of the screening population, 80 generations, 10 solutions, and an 8Å active site radius. Using the slow docking approach, the ligand was docked with each PDB file's binding site. Every pose's energy is determined by IGEMDOCK [35]. Ultimately, the output files that were received from iGEMDOCK as best posture and protein were displayed using DS visualizer.

For further confirmations of score obtained best pose obtained was redocked into extracted cavity of protein. To further confirm the potential of analogs as drug their drug safety profile were also studied along with reference compound 66 and curcumin.

Journal of Chemical Health Risks
www.jchr.org
JCHR (2025) 15(5), 465-493 | ISSN:2251-6727

2.4 Drug profile

Considering the important role of ADME and toxicity factors for drug safety, efficacy and compliance to regulatory standards it is important that they are assessed. Knowing how, where, and to what extent a drug is taken in, acted upon by the body, stored, and expelled; as well as recognizing the possibility of toxicity of such action helps in the improved and efficient development, formulation, and administration of medications and consequently, caring for patients. Although docking was performed for some promising analogs but for better understanding of their assimilation drug profile of all the analogs have been evaluated.

2.4.1 Probable drug properties

Molinspiration is a free online web server, was used to calculate probable drug properties calculates molecular properties using Java (http://www.molinspiration.com/). milogP (partition coefficient), TPSA (topological polar surface area), mass, HBA (number of hydrogen bond acceptor), HBD (number of hydrogen bond donor), and nrotb (rotatable bonds) and Molecular Volume (volume of drug distribution)[36]. Curcumin and its analogswere compared with standard antimalarial drugs Chloroquine and Artemether by processing one at a time, either with the SMILES code or by drawing their structures manually.

2.4.2 Bioactivity Score

In addition to using server molinspiration and drug-likeness properties to compare and validate the likelihood of analogs as an active compound, the bioactivity score of analoges against a variety of receptors, including GPCR (G-protein coupled receptor) ligand, ion channel modulator, kinase inhibitor, nuclear receptor ligand, protease inhibitor, and other enzyme inhibitors, was also calculated[37]

2.4.3 ADME properties

The requirement of molecule with strong pharmacodynamic and pharmacokinetic properties is the primary goal of the drug discovery phase. As a result, in order for an analog to be considered a potential drug, it must satisfy certain criteria, such as absorption, distribution, metabolism, and excretion, which decide the drug's biological effect[38].Various online web resources like vNN-ADMET[39] (https://vnnadmet.bhsai.org/vnnadmet/home.xhtml), SWISS ADME [40] (http://www.swissadme.ch/) and admetSAR [41](http://lmmd.ecust.edu.cn/admetsar2/) were used to measure some of the essential properties of selected probable drug candidates that obey Lipniki's law, such as Human Intestinal Absorption (HIA), Caco-2 Permeability, Plasma protein binding, Blood-Brain Barrier (BBB), Maximum Recommended Therapeutic Dose (MRTD), solubility, and bioavailability score.

2.4.4 Toxicity assessment

Toxicity profile of selected analogs with strong pharmacodynamic and pharmacokinetic properties was also assessed. The best analog for further analysis was chosen from a group of analogs with the least toxicity for humans and the environment[42]. To determine ADME properties, the software admetSAR was used (http://lmmd.ecust.edu.cn/admetsar1/predict/).

Journal of Chemical Health Risks

www.jchr.org

JCHR (2025) 15(5), 465-493 | ISSN:2251-6727

3. Results and Discussion

The purpose of the present study is to identify curcumin analogs as anti-falcipain compounds over cathepsin using *in-silico* studies. Falcipain is an important thiol protease found responsible for haemolysis of parasite, *Plasmodium falciparum*. The result can lead to effective antimalarial agents.

3.1 Determination ofSequence pair alignment and chemistry of both proteins

The aim of structure alignment is to identify the most corresponding pairs of amino acids that produce a good structural fit when the structures are overlaid **(Fig II)**. Results of flexible alignment of cathepsins B, H, and L with Falcipain-2 in terms of pair wise sequence alignment. In the alignment, we can observe the presence of cysteine residues in the following positions:

- Cathepsin L (3BC3_1|Chains): Cysteine residues are present at positions corresponding to "QCGSCW" and "GQCGGL" in the alignment.
- Cathepsin H (8PCH_1|Chain): Cysteine residues are present at positions corresponding to "GSCGSCW" and "GSCGSCW" in the alignment.
- Falcipain-2 (3BPF_1|Chains): Cysteine residues are present at positions corresponding to "QKNCGSCW" in the alignment.
- Cathepsin H (8PCH_2|Chain): Cysteine residues are present at positions corresponding to "EPQNCSAT" in the alignment.

```
2IPP_2|Chain      ------------------------------------------------------------ 0
2IPP_1|Chain      ------------------LPASFDAREQWPQCPTIKEIRDQGSCGSCWAFGAVEAISDRIC 43
3BC3_1|Chains     ------------------APRSVDWREKG----YVTPVKNQGQCGSCWAFSATGALEGQMF 39
8PCH_1|Chain      ------------------YPPSMDWRKKG---NFVSPVKNQGSCGSCWTFSTTGALESAVA 40
3BPF_1|Chains     QMNYEEVIKKYRGEENFDHAAYDWRLHS----GVTPVKDQKNCGSCWAFSSIGSVESQYA 56
8PCH_2|Chain      ----------------------------------------EPQNCSAT-------------- 8

2IPP_2|Chain      ----VSVEVSAEDLLTCCGSMCGDGCNGGYPAEAWNFWTRKGLV-SGGLYESHVGCRPYS 55
2IPP_1|Chain      IHTN------------------------------------------------------- 47
3BC3_1|Chains     RKTGRLISLSEQNLVDCSGPQGNEGCNGGLMDYAFQYVQDNGGLDSEESY-------PYE 92
8PCH_1|Chain      IATGKMLSLAEQQLVDCAQNFNNHGCQGGLPSQAFEYIRYNKGIMGEDTY-------PYK 93
3BPF_1|Chains     IRKNKLITLSEQELVDCS--FKNYGCNGGLINNAFEDMIELGGICPDGDY-------PYV 107
8PCH_2|Chain      ------------------------------------------------------------ 8

2IPP_2|Chain      IPPCEHHVNGSRPPCTGEGDTPKCSKICEPGYSPTYKQDKHYGYNSYSVSNSEKDIMAEI 115
2IPP_1|Chain      ------------------------------------------------------------ 47
3BC3_1|Chains     -------------------ATEES----C--KYNPKYSVANDTGFVDIP--KQEKALMKAV 126
8PCH_1|Chain      -------------------GQDDH----C--KFQPDKAIAFVKDVANIT-MNDEEAMVEAV 128
3BPF_1|Chains     -------------------SDAPN---LC--NIDRCTEK---YGIKNYL-SVPDNKLKEAL 140
8PCH_2|Chain      ------------------------------------------------------------ 8

2IPP_2|Chain      YKNGPVEGAFSV-YSDFLLYKSGVYQHVTGE---MMGGHAIRILGWGVEN---------- 161
2IPP_1|Chain      ------------------------------------------------------------ 47
3BC3_1|Chains     ATVGPISVAIDAGHESFLFYKEGIYFEPDCS--SEDMDHGVLVVGYGFEST------ESD 178
8PCH_1|Chain      ALYNPVSFAFEV-TNDFLMYRKGIYSSTSCHKTPDKVNHAVLAVGYGEEN---------- 177
3BPF_1|Chains     RFLGPISISVAV-SDDFAFYKEGIFDGEC----GDQLNHAVMLVGFGMKEIVNPLTKKGE 195
8PCH_2|Chain      ------------------------------------------------------------ 8

2IPP_2|Chain      GTPYWLVANSWNTDWGDNGFFKILRGQD----HCGIESEVVAGIPRTD      205
2IPP_1|Chain      ------------------------------------------------      47
3BC3_1|Chains     NNKYWLVKNSWGEEWGMGGYVKMAKDRR---NHCGIASAASYPTV---      220
8PCH_1|Chain      GIPYWIVKNSWGPQWGMNGYFLIERGKN----MCGLAACASYPIPLV-      220
3BPF_1|Chains     KHYYYIIKNSWGQQWGERGFINIETDESGLMRKCGLGTDAFIPLIE--      241
8PCH_2|Chain      ------------------------------------------------      8
```

Fig: II: Overlaid structure of chain A of fac-2(orange) over chain A of cathepsins (blue) a=CathB, b=CathH, c=CathL.

Journal of Chemical Health Risks

www.jchr.org

JCHR (2025) 15(5), 465-493 | ISSN:2251-6727

It appears that there are conserved cysteine residues in the aligned sequences, particularly in the regions corresponding to the catalytic domains or other functionally important regions. The presence of conserved cysteine residues suggests a potential functional similarity, as these residues may be involved in disulfide bond formation or other catalytic activities. The results also showed that chain A Falcipain-2 aligns Cath H, and L to great extent as topological similarity in terms of TM-score ranges near to 1 with low value of rmsd indicates better alignment[43]. The sequence similarity percentage between Falcipain-2 and Cathepsin B, H, and L is 58.14%, 57.42%, and 59.62% respectively. For more detail analysis of inhibition mechanism these proteins are investigated on the PrankWeb server, revealed more than one potential binding site with the ligands. Out of these predicted sites, the site with highest binding score i.e. respectively for protein with id 2IPP, 8PCH, 3BC3, and 3BPF possessing relatively high affinity to bind ligand **(Fig III)**. It was reported that CYS (acts as the nucleophile and forms a covalent bond with the substrate during catalysis) is the active site amino acid of catalytic site with HIS (Serves as a general base, accepting a proton from cysteine and facilitating the nucleophilic attack on the substrate) and ASN (Assists in the stabilization of the histidine residue, optimizing its ability to act as a general base) other two triad amino acid **Figure IV**.

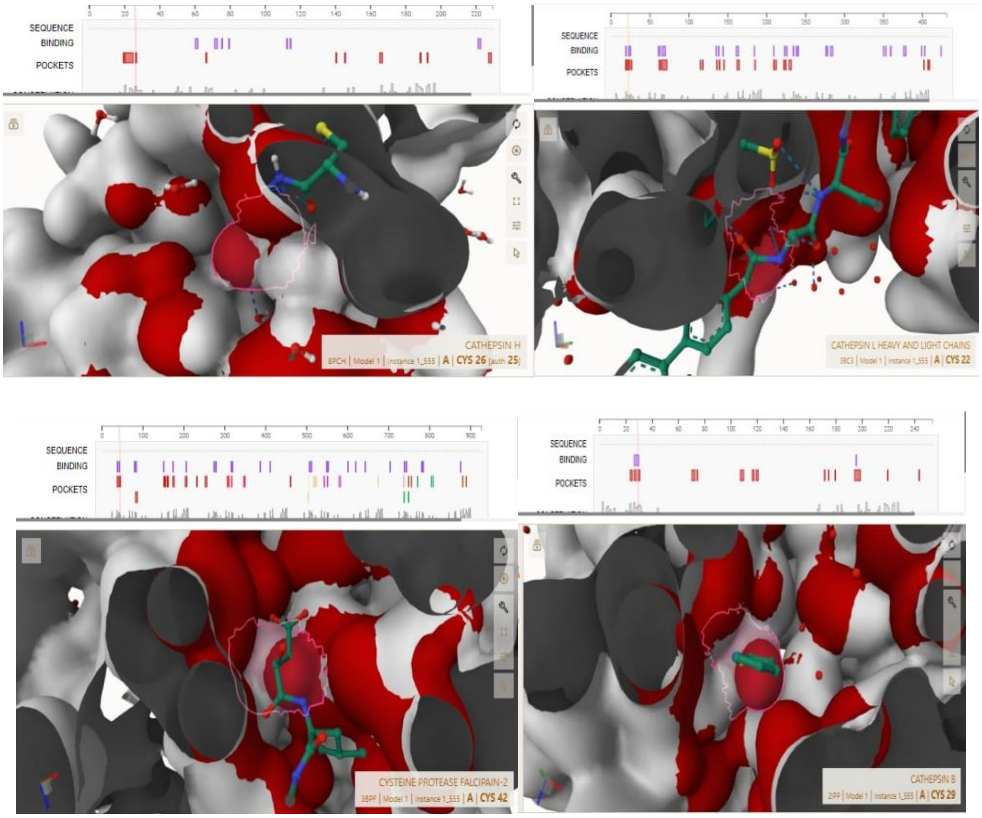

Fig III: Binding pocket images of cathepsin H, L,B and fac-2 involving cysteine residue

Journal of Chemical Health Risks

www.jchr.org

JCHR (2025) 15(5), 465-493 | ISSN:2251-6727

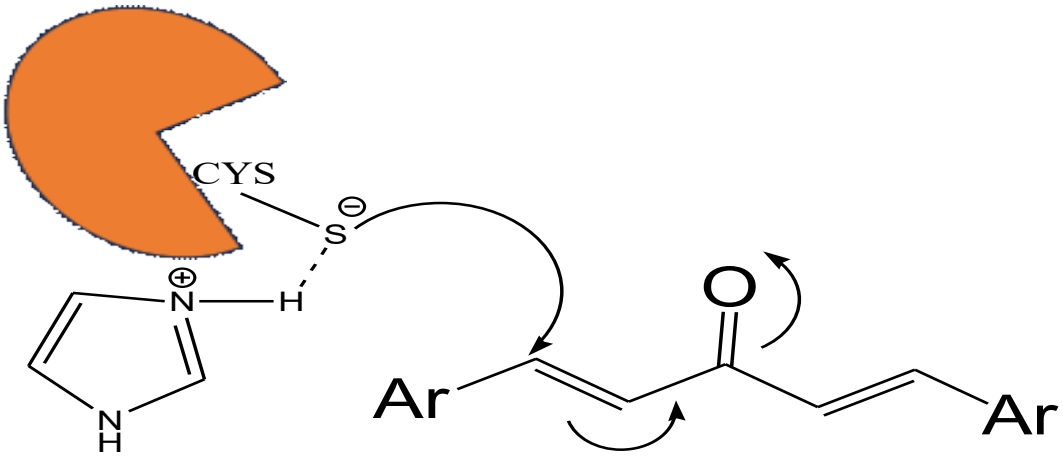

Figure IV: Interaction of active amino acid (CYS) with designed inhibitor

3.2 QSAR modelling

The Dragon descriptor calculation facility was used to calculate 1666 descriptors for each energy minimized compound. To lessen the redundancy in the descriptor dataset, the descriptor pool was first inspected. Descriptors with constant and almost constant values for all molecules were initially eliminated (1304 descriptors). Then, using the vWSP algorithm proposed by Ballabio et al. with cut-off values for variance and intercorrelation coefficient of 0.01 and 0.7, respectively, significantly inter correlated descriptors were eliminated (269 descriptors)[44]. Genetic algorithm was applied to reduced set of descriptors to select the most significant descriptors relevant to target value (log% inhibition). Here, a sequence of 269 genes representing the presence and absence of a descriptor was coded by 1 or 0 respectively. The presence of a few number of selected descriptors and a high value of fitness function in the chromosomes was considered as informative chromosomes. Finally, 10 descriptors showing high accordance with log% inhibition activity were selected these are as follows, MATS8e(2D autocorrelations): Moran autocorrelation of lag 8 weighted by Sanderson electronegativity, Hy(Molecular properties): hydrophilic factor, Mor29m(3D-MoRSE descriptors): signal 29 / weighted by mass, DISPe(Geometrical descriptors): displacement value / weighted by Sanderson electronegativity, RDF130u(RDF descriptors): Radial Distribution Function - 130 / unweighted, EEig09x(edge adjacency indices) : Eigenvalue 09 from edge adj. matrix weighted by edge degrees, RDF025e(RDF descriptors): Radial Distribution Function - 25 / weighted by Sanderson electronegativity, BELv5(Burden eigen value) : lowest eigenvalue n. 5 of Burden matrix / weighted by atomic van der Waals volumes, RDF070u(RDF descriptors): Radial Distribution Function - 70 / unweighted, MATS3m(2D autocorrelations): Moran autocorrelation of lag 3 weighted by mass.

Journal of Chemical Health Risks

www.jchr.org

JCHR (2025) 15(5), 465-493 | ISSN:2251-6727

Table I: Experimental and predicted Log% inhibition data for chalcones and designed compounds using10-4-1 ANN

S.No.	Comp. No.	log%inhibition(EXP.)	log%inhibition(pred)	S.No.	Comp. No.	log%inhibition(EXP.)	log%inhibition(pred)
Training set				Test Set			
1	2	0.7533	0.7696	1	1	-0.2424	-0.0093
2	3	0.443	0.6755	2	20	0.6075	0.898
3	4	0.0679	0.2921	3	23	1.0048	0.947
4	5	0.126	0.197	4	31	0.37	0.2065
5	6	-0.0295	0.0744	5	32	-0.1242	0.0837
6	7	0.4679	0.3782	6	41	0.565	0.6893
7	8	0.2442	0.2465	7	42	0.5967	0.8172
8	9	0.2784	0.1616	8	45	0.6734	0.7384
9	10	0.7671	0.6544	9	50	0.0452	0.0518
10	11	0.4543	0.5379	10	51	0.4298	0.3069
11	12	0.4543	0.5358	11	58	0.1491	0.0782
12	13	0.2612	0.1467	12	64	-0.3659	0.1264
13	14	0.3434	0.3117	13	69	-0.1617	0.0575
14	15	0.3394	0.2292	14	71	0.443	0.3262
15	16	0.5497	0.5357	15	73	0.3234	0.2333
16	17	0.1455	0.0691	16	77	0.4982	0.5332
17	18	0.2461	0.1498	17	80	0.6527	0.5586
18	19	0.2218	0.0839	Designed Compounds			
19	21	0.7137	0.5807	1	D1	_	-0.0071
20	22	0.3434	0.0963	2	D2	_	0.0302
21	24	0.8217	0.7668	3	D3	_	0.0127
22	25	0.7234	0.6947	4	D4	_	0.4586
23	26	0.1171	0.3187	5	D5	_	1.609
24	27	0.3495	0.2947	6	D6	_	0.9853
25	28	0.4232	0.4578	7	D7	_	0.0063
26	29	0.4232	0.4512	8	D8	_	0.0754
27	30	0.1047	0.3116	9	D9	_	1.5914
28	33	0	0.2691	10	D10	_	1.7646
29	34	1.4154	1.0887	11	D11	_	1.7646
30	35	0.6979	1.1197	12	D12	_	1.7645
31	36	0.4498	0.2977	13	D13	_	1.8222
32	37	0.4656	0.3399	14	D14	_	1.7647
33	38	0.187	0.3218	15	D15	_	1.0305

Journal of Chemical Health Risks

www.jchr.org

JCHR (2025) 15(5), 465-493 | ISSN:2251-6727

34	39	0.9215	0.1245
35	40	0.7365	0.8265
36	43	1.1102	0.7691
37	44	0.6185	0.8113
38	46	0.4543	0.2922
39	47	0.4702	0.4766
40	48	0.8217	0.7539
41	49	0.2708	0.1185
42	52	0.2688	0.2023
43	53	-0.0644	0.107
44	54	1.0911	0.283
45	55	0.1295	0.2976
46	56	0.3334	0.4863
47	57	0.8612	0.7849
48	59	0.5833	0.7947
49	60	0.1065	0.1776
50	61	0.6948	0.3985
51	62	0.3659	0.1897
52	63	-0.1348	0.0487
53	65	0.6213	0.4612
54	66	0.9943	0.8988
55	67	0.0924	0.3048
56	68	0.1331	0.3103
57	70	0.3805	0.1971
58	72	1.307	1.0508
59	74	0.6269	0.6208
60	75	0.5102	0.6798
61	76	0.7776	0.757
62	78	0.5548	0.6687
63	79	0.7848	0.5059
64	81	0.5396	0.6368
65	82	0.6158	0.7917

16	D16	_	1.0571
17	D17	_	1.5787
18	D18	_	1.8219
19	D19	_	2.0483
20	D20	_	1.0795
21	D21	_	0.0855
22	D22	_	0.2683
23	D23	_	1.1646
24	D24	_	1.8837
25	D25	_	1.5838
26	D26	_	2.0453
27	D27	_	2.0304
28	D28	_	0.8118

The correlation among selected descriptors was analyzed by computing the correlation matrix. No significant correlation is observed between the selected descriptors. These descriptors chosen by the genetic algorithm encode different aspects of the molecular structure like, hydrophilicity, geometrical aspect electro negativity, polarizability etc. It is important to note that factors such as shape, electro negativity, size, polarizability, hydrophilicity etc. affect, the binding mode of the inhibitor binds to the target site. These features are well taken into account by the descriptors chosen by GA. The complete

Journal of Chemical Health Risks

www.jchr.org

JCHR (2025) 15(5), 465-493 | ISSN:2251-6727

dataset (82 molecules) was divided into training and test sets using the Kennard-Stone approach. As a result, 65 compounds, or 80% of the data set, were used as the training set, and 17compounds, or 20%, were used as the test set for ANN implementation.

To investigate the non-linear relationship between descriptors and reported log% inhibition values of chalcones, three-layer backpropagation ANN models were built using GA selected ten descriptors used as input vectors[45]. The output layer's transfer function was linear, while the first layer's transfer function was tan-sigmoid. The idea of ρ presented by Andrea and Kalayeh was utilized to optimize the number of nodes in the hidden layer.By adjusting the number of nodes 3 to 6 in the hidden layer, the MSE value for the test set was calculated.The network of 10-4-1 was ultimately chosen, after several training sessions on the basis of low MSE value for the test set. Table 1 shows the predicted log% inhibition values for the training and test sets.

External validation

External validation (using an independent test set) is commonly used to assess the accuracy of a QSAR model's predictions. Various validation metrics, such as R^2 based metrics such as R^2test, Q^2(ext F1), Q^2(ext F2), average R^2m, ΔR^2m, and so on, and error-based measures such as root mean square error (rmse), SD(standard deviation), mean absolute error (mae), etc were computed and analyzed. The performance was also verified by computing parameters suggested by Golbraikh and Tropsha and Grammatica *et al*. All parameters are presented in **Table II**. The calculated values of these parameters are in good agreement with the proposed criteria confirming the reliability of the proposed model, as reported in the **table1**, predicted values are very close to the experimental values.

Table II: Statistical parameters for test set

r^2=	0.765457	r0^2=	0.7494
mse	0.036631	SD=	0.1178
rmse	0.191391	Q2f1=	0.7704
mae	0.1535	Q2f2=	0.7299
k=	0.898078	rm^2=	0.5997
k'=	0.955113	Δrm^2=	0.2
R02=	0.973938	CCC=	0.8486
R'02=	0.996448		

The % inhibition value of some compounds having heteroatom like 48, 54 and especially 66, is quite high. Based on this observation, we have designed new E-chalcones **(Table III)** with heterocyclic moiety and used them as external test set. The developed and thoroughly validated GA and ANN model was used to predict respective log% inhibition activity of 28 newly designed compounds. The predicted values for the external test set were according to the expectations (-0.0071 to 2.0483). The presence of heterocyclic moiety in these analogs makes them more potent inhibitors with high log% inhibitors (predicted) values. Encourage by their QSAR predictions we also studied modelling interaction and drug profile of some promising candidate to check their emergence as potent drug.

Journal of Chemical Health Risks

www.jchr.org

JCHR (2025) 15(5), 465-493 | ISSN:2251-6727

Table III: Designed Analogs

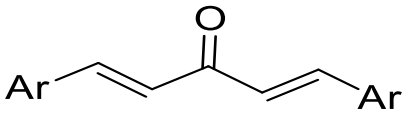

Compound	Ar group	Compound	Ar group
D1	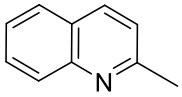	**D15**	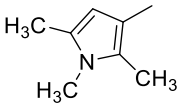
D2	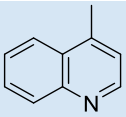	**D16**	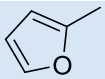
D3	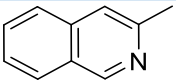	**D17**	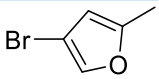
D4	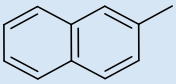	**D18**	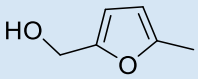
D5	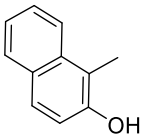	**D19**	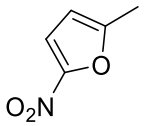
D6	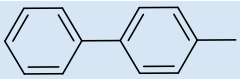	**D20**	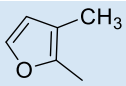
D7	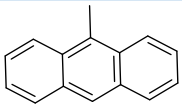	**D21**	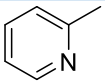
D8	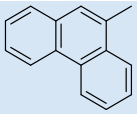	**D22**	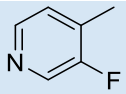
D9	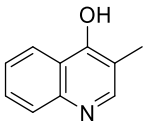	**D23**	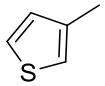
D10	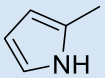	**D24**	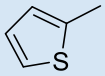

Journal of Chemical Health Risks
www.jchr.org
JCHR (2025) 15(5), 465-493 | ISSN:2251-6727

D11	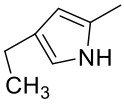	**D25**	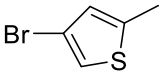
D12	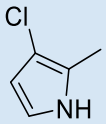	**D26**	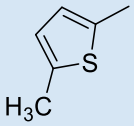
D13	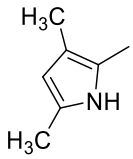	**D27**	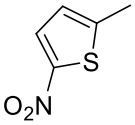
D14	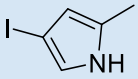	**D28**	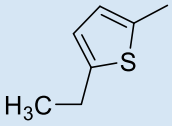

3.3 Molecular Docking

For selecting one best analog, above screened both analogs were compared with parent compound curcumin, one of the compounds with high % inhibitions66and standard drugs chloroquine, artemether in terms of affinity for cathepsins B, H, L, and Fac-2 by docking using Autodock vina which was further revalidated by using iGemdock docking software. Release in energy after interactions of standard drug, curcumin, reference 66 and screened analogs with cathepsins, and fac-2 shows that analogs are well-fitted in the receptor cavity and binds well. Out of 9 poses obtained in each case the pose with maximum release of energy was chosen as best pose, results of which are as shown in **figure V** in terms of bar graph. On the basis of interaction data of docking experiments (bar graph), it was observed that Analog D9 shows the maximum affinity of -104.757kcal/mol which of value compared to reported reference compound 66. Additionally, the contribution of Vanderwall interactions is more with score -88.6669 kcal/mol as compared to H-bond with score -16.0903kcal/mol for Fac-2 even more than standard antimalarial drug chloroquine and artemether. Also, among the screened compounds, we identified that our selected analogs exhibited strong binding affinity specifically towards the active site of falcipain while showing limited interaction with the active site of cathepsin. Interestingly, designed analog D9 and D10 emerged as a promising candidate, demonstrating robust interactions with critical residues within the falcipain active site. These interactions include hydrogen bonding, hydrophobic contacts, and π-π stacking interactions, suggesting a high degree of specificity for falcipain. The overall result suggested the selective inhibition of falcipain over cathepsin which is crucial for minimizing potential side effects in the host. Compound D9 and D10 are suitable drug candidates as antimalarial compounds in terms

Journal of Chemical Health Risks

www.jchr.org

JCHR (2025) 15(5), 465-493 | ISSN:2251-6727

of falcipain inhibitors. While considering the structure similarity between these two molecules, we find that nitrogen is present in both the compounds. Further, compound D9 is having the similar scaffold as that present in standard drug chloroquine shows maximum affinity towards target protein **(figure VI)**. Both compounds D9 and D10 contain similar site of action as that present in curcumin.

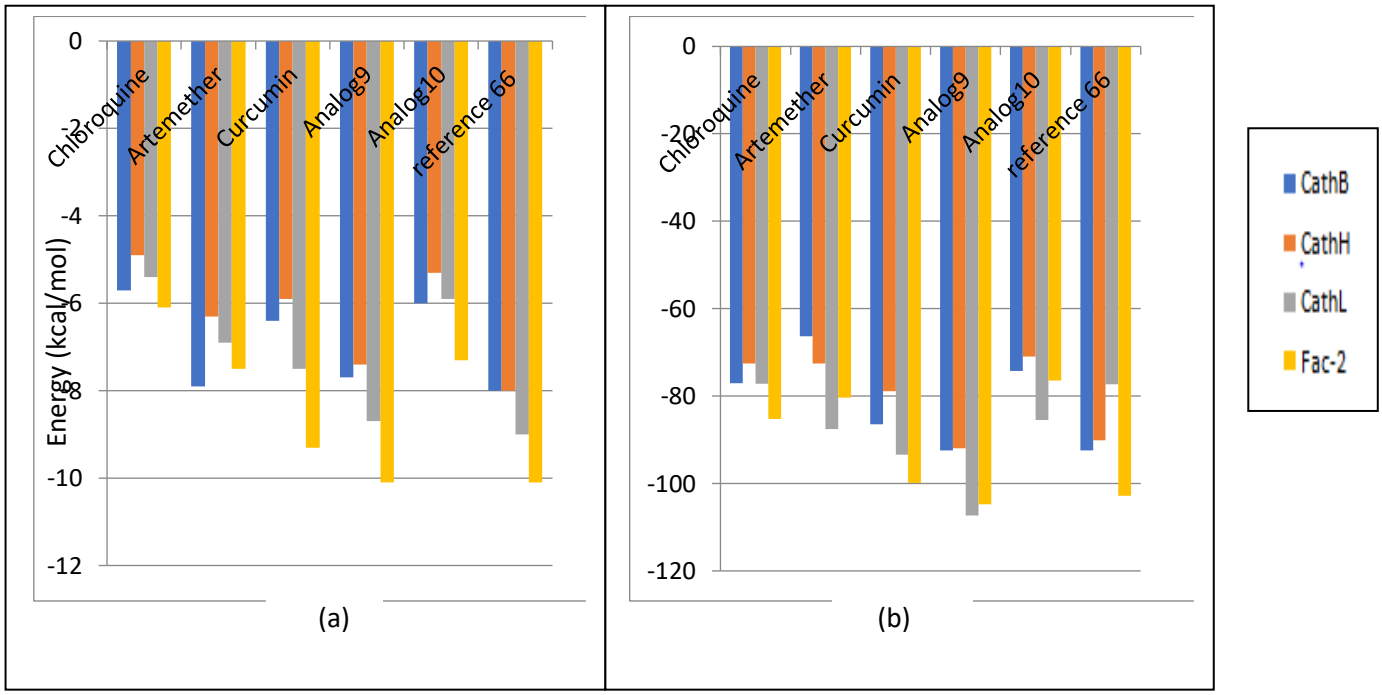

Figure V: Energy profile (a) by Autodock (b) By igemdock

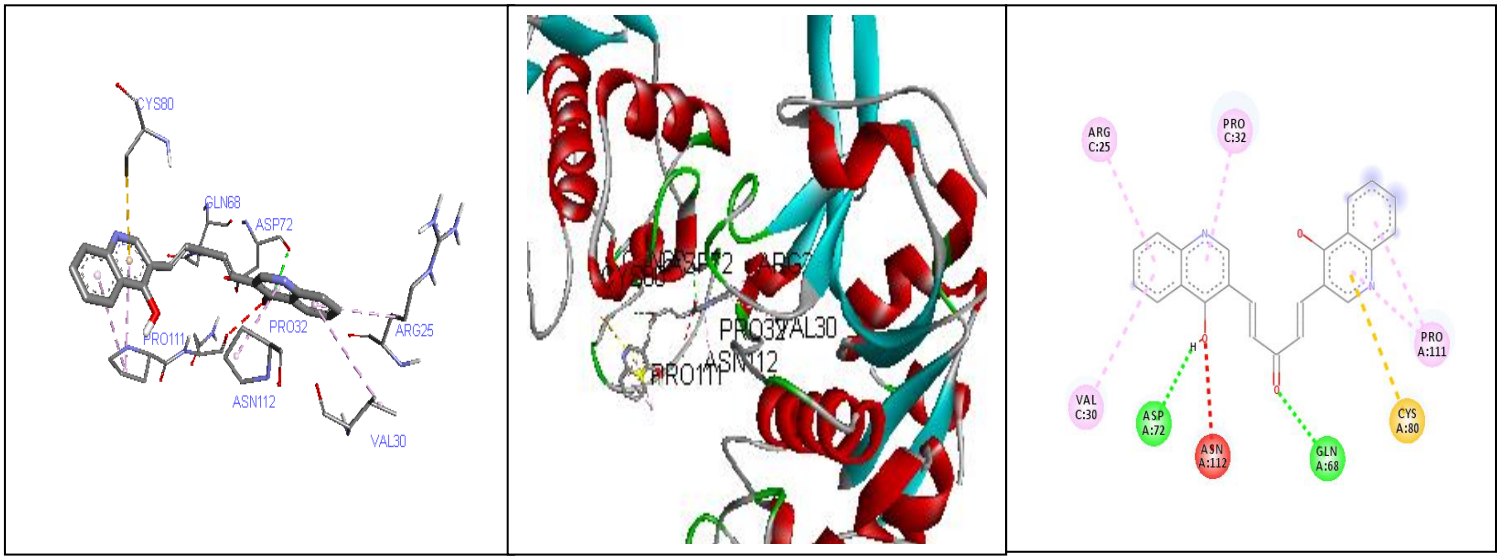

Figure VI: Interaction of analaogD9 with falcipain

Journal of Chemical Health Risks

www.jchr.org

JCHR (2025) 15(5), 465-493 | ISSN:2251-6727

3.4 Probable drug profile

If compounds with physicochemical parameters that are compatible with transport to the target site are chosen for screening, the probability of them being discovered as drugs increases. The oral bioavailability of drugs has been linked to a set of basic parameters (molecular mass, log P, hydrogen bond donors and acceptors, rotatable bonds). Calculated properties based on molecular structure of all designed analogs using molinspiration are compiled in **table IV**. Standard drug Chloroquine and 7 analogs shows 1 violation for lipnikis rule whereas, Lipophilicity measured parameter i.e. milogP lies in range 1 to 5, for rest of the analogs. The M.W of analogs <500g/mol with the number of hydrogen donor and acceptor atoms in range i.e. <5 and <10 respectively. All screened analogs have parameter that correlated with flexibility i.e. rotable bonds in acceptable range of <10. In addition, one more parameter in terms of polar surface area correlated with permeability and interactions lies in required range $<140A^0$ [46].

Table IV: Probable drug properties.

Compound	miLogP	TPSA	natoms	MW	nON	nOHNH	nrotb	Vol.	Violation
Chloroquine	**5.00**	28.16	22	319.88	3	1	8	313.12	1
Artemether	3.40	46.17	21	298.38	5	0	1	281.62	0
Curcumin	3.05	96.22	27	368.38	3	6	7	331.83	0
D1	3.98	42.85	26	336.39	3	0	4	308.94	0
D2	4.30	42.85	26	336.39	3	0	4	308.94	0
D3	4.96	42.85	26	336.39	3	0	4	308.94	0
D4	**6.55**	17.07	26	334.42	1	0	4	317.25	1
D5	**6.30**	57.53	28	366.42	3	2	4	333.29	1
D6	**7.78**	17.07	30	386.49	1	0	6	372.09	1
D7	**8.35**	17.07	34	434.54	1	0	4	405.24	1
D8	**8.35**	17.07	34	434.54	1	0	4	405.24	1
D9	3.82	83.31	28	368.39	5	2	4	324.98	0
D10	2.13	48.65	16	212.25	3	2	4	199.24	0
D11	3.77	48.65	20	268.36	3	2	6	265.97	0
D12	3.35	48.65	18	281.14	3	2	4	226.31	0
D13	3.33	48.65	20	268.36	3	2	4	265.48	0
D14	4.16	48.65	18	464.04	3	2	4	247.22	0
D15	2.53	26.94	22	296.41	3	0	4	299.37	0
D16	2.34	43.35	16	214.22	3	0	4	192.41	0
D17	3.81	43.35	18	372.01	3	0	4	228.18	0
D18	1.49	83.81	20	274.27	5	2	6	242.04	0
D19	2.50	135	22	304.21	9	0	6	239.07	0

Journal of Chemical Health Risks

www.jchr.org

JCHR (2025) 15(5), 465-493 | ISSN:2251-6727

D20	3.09	43.35	18	242.27	3	0	4	225.53	0
D21	1.48	42.85	18	236.27	3	0	4	220.96	0
D22	1.87	42.85	20	272.25	3	0	4	230.82	0
D23	3.00	17.07	16	246.36	1	0	4	210.69	0
D24	3.62	17.07	16	246.36	1	0	4	210.69	0
D25	**5.10**	17.07	18	404.15	1	0	4	246.46	1
D26	4.07	17.07	18	274.41	1	0	4	243.81	0
D27	3.79	108.72	22	336.35	7	0	6	257.36	0
D28	**5.21**	17.07	20	302.46	1	0	6	277.42	1

3.4.1 Bioactivity Score

The potential effects of drugs in living organisms are defined by pharmacological action. A biological target is expected to bind to the drug. Enzymes, receptors, ion channels, and other proteins are common biological targets. Potential of analogs that follow Lipinski's rule for these targets determined in terms of biological activity is compiled in **table V**. It is known that; the compound is active if the bioactivity score is greater than 0.0; reasonably active if the bioactivity score is between -5.0 and 0.0; and inactive if the bioactivity score is less than -5.0 [47]. Like standard antimalarial drug and curcumin our screened analogs shows moderate to

Table V: Bioactivity score.

Compound	GPCR ligand	Ion Channel Modulator	Kinase Inhibitor	Nuclear Receptor Ligand	Proteases Inhibitor	Enzyme Inhibitor
Chloroquine	0.32	0.32	0.38	-0.19	0.05	0.11
Artemether	-0.05	-0.22	-0.44	-0.01	-0.07	0.45
Curcumin	-0.06	-0.20	-0.26	0.12	-0.14	0.08
D1	0.14	-0.12	0.05	-0.04	0.07	0.21
D2	0.06	-0.07	0.11	0.06	0.09	0.18
D3	0.18	0.05	0.19	-0.11	0.19	0.26
D9	0.07	0.01	0.17	0.13	0.04	0.28
D10	-0.23	-0.28	-0.32	-0.52	-0.56	0.17
D11	0.10	-0.17	-0.03	-0.24	-0.23	0.26

Journal of Chemical Health Risks
www.jchr.org
JCHR (2025) 15(5), 465-493 | ISSN:2251-6727

D12	-0.11	-0.18	-0.10	-0.29	-0.30	0.15
D13	-0.15	-0.36	-0.01	-0.26	-0.37	0.02
D14	-0.15	-0.29	-0.25	-0.35	-0.42	0.13
D15	-0.25	-0.64	-0.52	-0.25	-0.45	-0.10
D16	-0.71	-0.85	-0.93	-0.61	-0.85	-0.30
D17	-0.64	-0.69	-0.73	-0.47	-0.70	-0.19
D18	-0.34	-0.58	-0.42	-0.12	-0.33	0.0
D19	-0.56	-1.04	-0.49	-0.64	-0.58	-0.25
D20	-0.38	-0.69	-0.60	-0.32	-0.55	-0.17
D21	-0.03	-0.14	-0.10	-0.30	-0.15	0.23
D22	0.02	-0.07	-0.09	-0.08	-0.14	0.17
D23	-0.41	-0.49	-0.66	-0.39	-0.49	-0.07
D24	-0.62	-0.61	-0.59	-0.54	-0.57	-0.19
D26	-0.44	-0.52	-0.41	-0.31	-0.45	-0.14
D27	-0.45	-0.59	-0.34	-0.26	-0.34	-0.18

3.4.2 ADME properties

ADME properties have been identified as a significant cause of drug candidate failure in late-stage drug production that affects financial liability on the pharmaceutical industry's Research and development activities. Thus ADME properties are significant to measure before synthesis trial of the drug[48]. ADME properties such as Human Intestinal Absorption (HIA), Caco-2 Permeability, Plasma protein binding, Blood-brain barrier (BBB), Maximum recommended therapeutic dose (MRTD), solubility, and bioavailability score covering pharmacokinetics properties of compounds are compiled in **table VI**. Results shows that all the screened analogs including parent compound curcumin show positive prediction like standard drug for human intestinal absorption, human oral bioavailability, and comparable topological surface area suggesting effective assimilation by human intestine and good absorption **(Fig VII).** 16 analogs out of 21 selected analogs have positive prediction for Caco-2 permeability. Except D9 analogs all other shows less affinity than standard drug Chloroquine and Artemether for plasma protein binding

Journal of Chemical Health Risks

www.jchr.org

JCHR (2025) 15(5), 465-493 | ISSN:2251-6727

resulting in high amount of drug available to reach the target. The BBB of a drug is another important parameter that can help to minimize adverse effects and toxicity while also improving drug effectiveness. Most of the analog exhibit similar profile for BBB, P-glycoprotein inhibition, Cyp inhibition as both standard drugs. Results suggested that issue related to bioavailability of curcumin and analogs are not that significant as both the standard drugs exhibit equal bioavailability score to that of analogs with most of the analogs having greater aqueous solubility. One another important property that decides the effectiveness of drug with minimum quantity is MRTD value of that drug. Computationally determined MRTD value of curcumin is 650g/day that is higher than both the standard antimalarial drug i.e. 430g/day, 169g/day for chloroquine and artemether respectively but most of the analogs exhibited either comparable or better pharmacokinetic profile than standard drug with 13 of them having MRTD value lies in range between the two. These are further screened for toxicology studies to choose one best analog which lie in line of probable antimalarial drug.

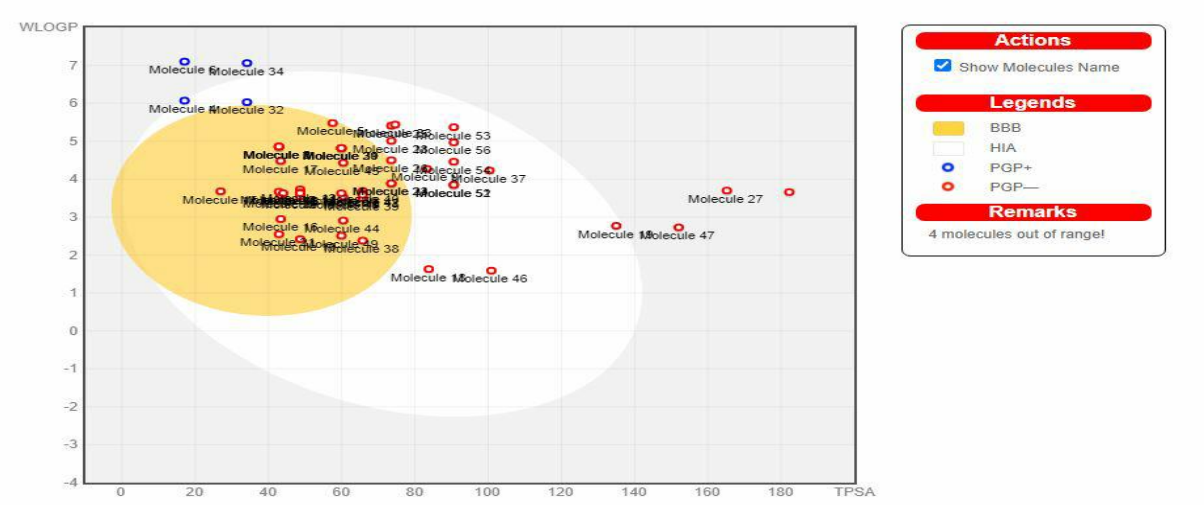

Fig VII: BOILED Egg graph of selected ligands allows for the evaluation of drug candidates for development by predicting the passive gastrointestinal absorption (HIA) and brain access of small molecules (BBB) in function of the orientation of the molecules in WLOG vs. tPSA plot

Table VI: ADME properties.

Name of Ligand	Human Intestinal	Caco-2 Permeability	%Ab=109-	Human oral	Plasma protein binding	BBB	P-glycoprotein inhibitors	Cyp1A2 Inhb	Cyp3A4 Inhb	Cyp2D6 Inhb	Cyp2C9 Inhb	Cyp2C19 Inhb	Bio. Score	Water Solubility (LogS)	MRTD (mg/day)

Journal of Chemical Health Risks

www.jchr.org

JCHR (2025) 15(5), 465-493 | ISSN:2251-6727

D12	D11	D10	D9	D3	D2	D1	Curcumin	Artemether	Chloroquine
+0.9780	+0.9874	+0.9763	+0.9758	+0.9800	+0.9800	+0.9800	+0.9770	+0.8171	+0.9963
+0.6244	+0.5705	+0.7508	-0.6930	-0.6438	-0.5563	-0.6356	-0.7658	+0.8599	+0.6682
92.21	92.21	92.21	80.25	94.21	94.21	94.21	75.80	93.07	99.28
+0.5714	+0.5286	+0.6571	+0.5143	+0.6143	+0.6571	+0.600	+0.6000	+0.8000	+0.8143
0.889	0.507	0.323	1.1.07	0.701	0.776	0.755	0.832	1.107	0.862
+0.9798	+0.9937	+0.9950	+0.8744	+0.9942	+0.9942	+0.994	-0.2466	+0.9536	+1.0000
-0.9331	-0.7311	-0.9537	-0.5514	-0.5891	-0.5635	-0.5964	+0.5967	-0.7903	-0.8404
+0.7877	+0.5205	-0.5384	+0.8766	+0.9265	+0.9265	+0.9265	+0.9106	+0.6829	-0.8586
-0.6463	-0.6756	-0.8579	-0.5460	-0.5417	-0.5417	-0.5417	-0.5392	-0.9434	-0.8308
-0.8047	-0.6532	-0.7778	-0.7371	-0.8764	-0.8764	-0.8764	+0.6715	-0.9474	-0.9218
-0.6794	-0.6223	-0.6083	+0.6835	-0.8037	-0.8037	-0.8037	+0.6796	-0.9413	-0.9071
+0.5078	-0.6454	-0.7523	+0.6800 9	+0.5451	+0.5451	+0.5451	+0.8994	-0.8733	-0.9025
0.55	0.55	0.55	0.55	0.55	0.55	0.55	0.56	0.55	0.55
-3.389	-1.307	-0.602	-4.04	-2.99	-2.99	-2.99	-3.364	-4.702	-4.348
145	116	112	235	198	56	3416	650	169	430

Journal of Chemical Health Risks

www.jchr.org

JCHR (2025) 15(5), 465-493 | ISSN:2251-6727

D23	D22	D21	D20	D19	D18	D17	D16	D15	D14	D13
+0.9546	+0.9677	+0.9663	+0.9832	+0.9064	+0.9631	+0.9597	+0.9701	+0.9863	+0.9490	+0.9872
+0.8579	+0.8662	+0.7411	+0.9140	-0.5214	-0.6074	+0.6406	+0.8225	+0.9195	+0.6449	+0.7544
83.62	94.21	94.21	94.04	62.42	80.08	94.04	94.04	99.70	92.21	92.21
+0.6286	+0.7143	+0.6714	+0.7286	+0.7714	+0.5571	+0.7286	+0.7286	+0.6000	+0.6143	+0.5857
0.638	0.604	0.373	0.894	0.911	0.692	0.924	0.606	0.845	0.643	0.843
+0.9905	+0.9814	+0.9949	+0.9826	+0.9744	+0.9627	+0.9816	+0.9827	+0.9956	+0.9895	+0.9924
-0.9439	-0.6937	-0.9346	-0.7940	-0.8760	-0.8070	-0.8440	-0.8966	-0.6883	-0.9172	-0.7821
+0.5094	+0.8920	+0.9145	+0.6857	+0.7033	-0.6377	-0.5060	-0.5268	+0.5294	+0.5957	+0.8509
-0.9605	+0.8125	-0.5904	-0.8973	-0.8113	-0.9430	-0.8486	-0.9517	-0.6640	-0.6944	-0.6104
-0.8394	-0.8422	-0.8255	-0.9374	-0.8852	-0.9464	-0.8795	-0.9285	-0.7953	-0.7795	-0.7580
-0.8098	+0.5763	-0.7848	-0.8385	-0.8294	-0.8850	-0.7318	-0.8948	-0.7528	-0.7049	-0.5424
-0.5000	+0.7193	-0.6420	-0.5793	-0.7375	-0.8159	+0.5208	-0.6797	-0.6364	-0.6701	+0.5665
0.55	0.55	0.55	0.55	0.55	0.55	0.55	0.55	0.55	0.55	0.55
-1.067	-3.32	-1.634	-1.842	-2.564	-0.507	-2.734	-1.161	-1.688	-2.778	-1.918
925	169	1374	1460	511	192	206	1246	174	240	145

Journal of Chemical Health Risks

www.jchr.org

JCHR (2025) 15(5), 465-493 | ISSN:2251-6727

D24	+0.9546	+0.8479	83.62	+0.6714	0.669	+0.9884	-0.9464	+0.5312	-0.9458	-0.8217	-0.7153	+0.5844	0.55	-1.028	1432
D26	+0.9759	+0.8632	83.62	+0.7429	0.845	+0.9892	-0.8934	+0.5399	-0.8977	-0.8374	-0.6598	+0.5772	0.55	-1.779	182
D27	+0.8808	+0.5666	52.00	+0.8143	0.826	+0.9736	-0.8926	+0.7442	-0.6527	-0.9000	-0.7461	-0.5349	0.55	-2.791	565

3.4.2Toxicity assessment

Computational toxicology is a growing field that combines evidence and knowledge from a range of sources to create statistical and computer-based models to help explain and forecast the negative health consequences of chemicals like environmental toxins and pharmaceuticals. The selceted analog must also posess great safety profile for envirnment, human body thus analogs was further screened for computational toxicology. Resluts obtained from admetSAR online server are compled in **table VII**. Analogs D16, D17, D18,and D19 shows warning or danger for carcinogeniity thus dropped out of the selection.Out of analogs with MRTD value in range between the two standard drug , most of the analogs shares comparable or less toxic profile than stabdard drugs. We conclude that anlaog D9 and D10 are best analogs with only two toxicity prediction whereas chloroquine shows 5 and armether shows 3 positive predictions for toxic effects on human and environment.

Table VII: Toxicity assessment

Type of toxicity	**Organ toxicity**					**Genomic toxicity**			**Eco-toxicity**			
Name of ligand	**Human either-a-go-go inhibition**	**Hepatotoxicity**	**Acute Oral Toxicity (c)**	**Eye corrosion**	**Eye irritation**	**Ames mutagenesis**	**Carcinogenicity (binary)**	**Carcinogenicity (trinary)**	**crustacea aquatic toxicity**	**Biodegradation**	**Fish aquatic toxicity**	**Honey bee toxicity**

Journal of Chemical Health Risks

www.jchr.org

JCHR (2025) 15(5), 465-493 | ISSN:2251-6727

D12	D11	D10	D9	D3	D2	D1	Curcumin	Artemether	Chloroquine
-0.5919	+0.8464	-0.5990	-0.4654	+0.7361	+0.6451	+0.7412	-0.4263	-0.6016	+0.9368
+0.8000	+0.7000	+0.6750	+0.7750	+0.7250	+0.7750	+0.8000	+0.7250	-0.7750	+0.5500
II 0.4793	III 0.6702	III 0.5427	III 0.4700	III 0.6078	III 0.6078	III 0.6078	III 0.6349	IV 0.4732	II 0.7370
-0.9338	-0.9719	-0.7554	-0.9955	-0.9719	-0.9719	-0.9719	-0.9778	-0.9812	-0.9886
+0.7001	-0.5855	+0.9564	-0.6389	-0.5828	+0.6044	-0.5282	+0.7044	-0.9015	-0.9774
-0.8100	-0.7400	-0.7300	-0.5300	-0.7300	-0.6400	-0.6300	-0.9600	-0.6900	+0.7000
-0.7800	-0.8031	-0.7800	-0.8030	-0.7453	-0.7881	-0.7453	-0.8061	-0.9286	-0.8286
Non-required	Non-required	Non-required	Non-required	Non-required	Non-required	Non-required	Non-required	Non-required	Non-required
+0.5049	-0.6752	-0.6600	-0.6900	-0.5900	-0.6400	-0.6700	-0.6400	+0.6600	+0.8900
-0.7500	-0.8750	-0.7500	-0.9500	-0.9250	-1.0000	-0.9250	-0.8000	-0.8000	-0.8750
+0.7831	-0.6476	-0.7268	+0.7341	-0.6574	-0.6574	-0.6574	+0.9787	+0.8648	+0.9880
-0.5502	+0.5593	-0.4903	-0.4885	+0.5255	+0.5255	+0.5255	+0.5467	+0.7922	-0.7649

Journal of Chemical Health Risks

www.jchr.org

JCHR (2025) 15(5), 465-493 | ISSN:2251-6727

D23	D22	D21	D20	D19	D18	D17	D16	D15	D14	D13
-0.6219	+0.6978	-0.6247	-0.4112	-0.8167	-0.3915	+0.7477	-0.5375	-0.3876	-0.4550	+0.6708
+0.7250	+0.7750	+0.7250	+0.7250	+0.7750	+0.6750	+0.6250	+0.6750	+0.8000	+0.6500	+0.9000
III 0.7427	III 0.4503	III 0.5625	III 0.7621	III 0.5964	III 0.7218	III 0.7748	III 0.7155	III 0.5208	III 0.4571	III 0.6431
+0.6534	-0.9447	-0.9409	-0.7770	-0.9333	-0.9253	+0.6632	+0.7076	-0.9187	-0.8726	-0.9740
+0.9735	-0.5697	+0.9277	+0.7813	-0.5616	-0.5720	+0.7643	+0.9614	+0.5670	-0.8020	-0.4790
-0.8900	-0.7700	-0.8300	-0.7200	+0.9900	-0.6400	-0.7600	-0.8700	-0.7700	-0.7900	-0.6200
-0.7602	-0.7596	-0.7055	-0.6776	-0.6459	-0.6943	-0.6800	-0.6800	-0.7061	-0.7800	-0.7633
Non-required	Non-required	Non-required	Non-required	Danger	Danger	Danger	Warming	Non-required	Non-required	Non-required
-0.6100	-0.6000	-0.6600	-0.7500	-0.8800	-0.7600	-0.6100	-0.7600	-0.6684	-0.6600	-0.5900
-0.7000	-0.8750	-0.9000	-0.7500	-0.9250	-0.9000	-0.9000	-0.7250	-0.9250	-0.9000	-0.9000
+0.8047	+0.8288	-0.7006	+0.9068	+0.8539	-0.6250	+0.9319	+0.7537	-0.5768	-0.3976	-0.4409
+0.7446	-0.5886	-0.6124	+0.6483	-0.7301	-0.4852	+0.7177	+0.6511	+0.5330	-0.4932	+0.5615

Journal of Chemical Health Risks

www.jchr.org

JCHR (2025) 15(5), 465-493 | ISSN:2251-6727

D24	-0.5787	+0.7000	III 0.6895	+0.5438	+0.9665	-0.8400	-0.7602	Non-required	-0.6100	-0.7250	+0.8737	+0.7810
D26	+0.7114	+0.7250	III 0.9042	-0.6930	+0.8347	-0.7800	-0.7745	Non-required	-0.6700	-0.8750	+0.8910	+0.7996-
D27	-0.7738	+0.8250	III 0.5371	-0.9025	-0.6156	+0.8200	-0.6888	Non-required	-0.7900	-0.8750	+0.9639	-0.5288

Conclusion

The study integrates computational techniques for selecting optimal analog of curcumin for falcipain-2 inhibition over cathepsins to emerge as a potent drug with good drug safety profile. In the present study homology between cathepsins and falcipain-2 encourages us to look for cathepsins inhibitors as future antimalarial drug. In conclusion, the research has identified the designed analogs D9 and D10 as promising falcipain inhibitors by predicting their promising log% inhibition values of 1.59 and 1.76, respectively, based on the QSAR well-developed model. Further docking interactions confirms analog D9 with a favorable binding profile with affinity of -104.757kcal/mol for target protein fal-2 and selectivity over cathepsin. Along with good % inhibition and great binding affinity for falcipain these found to have low toxicity along with Great ADME profile. This finding lays the groundwork for further optimization and development of novel antimalarial agents targeting falcipain, thereby contributing to the ongoing efforts to combat malaria.

Refrences

1. Weatherall, D. J., Abdalla, S., & Pippard, M. J. (1983). The anaemia of Plasmodium falciparum malaria. *Malaria and the Red Cell*, 74-87.
2. Cummings, J. F., Polhemus, M. E., Kester, K. E., Ockenhouse, C. F., Gasser Jr, R. A., Coyne, P., ... & Heppner, D. G. (2024). A phase IIa, randomized, double-blind, safety, immunogenicity and efficacy trial of Plasmodium falciparum vaccine antigens merozoite surface protein 1 and RTS, S formulated with AS02 adjuvant in healthy, malaria-naïve adults. *Vaccine*.
3. Wang, Z. (2024). Assessment of the long-term efficacy of the R21 malaria vaccine in African children. *Infectious Diseases and Microbiology*, *2*(1), 33-42.
4. Kumar, Y., Jain, A., & Kumar, R. (2023). Limitations of Current Drugs and Prospects of Plant-Based Compounds and Their Constructed Analogs as Therapeutics for Treatment of Malaria. In *Natural Product Based Drug Discovery Against Human Parasites: Opportunities*

and Challenges (pp. 451-469). Singapore: Springer Nature Singapore.

5. Agu, P. C., &Obulose, C. N. (2024). Piquing artificial intelligence towards drug discovery: Tools, techniques, and applications. *Drug Development Research*, *85*(2), e22159.
6. Al-Mohaya, M., Mesut, B., Kurt, A., & Çelik, Y. S. (2024). In silico approaches which are used in pharmacy. *Journal of Applied Pharmaceutical Science*, *14*(4), 239-253.
7. Pandey, V., Sharma, K., & Raghav, N. (2022). Ligand-based modeling of semicarbazones and thiosemicarbazones derivatives as Cathepsin B, H, and L inhibitors: A multi-target approach. *Journal of Molecular Structure*, *1257*, 132612.
8. Sharma, K., & Raghav, N. (2021). Curcumin analogs as anti-cathepsins agents: Designing, virtual screening, and molecular docking analysis. *Computational Toxicology*, *19*, 100174.
9. Mahanta, P. J., &Lhouvum, K. (2024). Plasmodium falciparum Proteases as new drug targets with special focus on Metalloproteases. *Molecular and Biochemical Parasitology*, 111617.
10. Rosenthal, P. J. (2020). Falcipain cysteine proteases of malaria parasites: An update. *Biochimica et Biophysica Acta (BBA)-Proteins and Proteomics*, *1868*(3), 140362.
11. Musyoka, T. M., Njuguna, J. N., &Tastan Bishop, Ö. (2019). Comparing sequence and structure of falcipains and human homologs at prodomain and catalytic active site for malarial peptide based inhibitor design. *Malaria Journal*, *18*, 1-21.
12. Scarcella, M., d'Angelo, D., Ciampa, M., Tafuri, S., Avallone, L., Pavone, L. M., & De Pasquale, V. (2022). The key role of lysosomal protease cathepsins in viral infections. *International journal of molecular sciences*, *23*(16), 9089.
13. Raghav, N., & Singh, M. (2014). Design, synthesis and docking studies of bischalcones based quinazoline-2 (1H)-ones and quinazoline-2 (1H)-thiones derivatives as novel inhibitors of cathepsin B and cathepsin H. *European Journal of Pharmaceutical Sciences*, *54*, 28-39.
14. Raghav, N., & Singh, M. (2014). SAR studies of differently functionalized chalcones based hydrazones and their cyclized derivatives as inhibitors of mammalian cathepsin B and cathepsin H. *Bioorganic & medicinal chemistry*, *22*(15), 4233-4245.McKerrow, J. H., Rosenthal, P. J., Swenerton, R., & Doyle, P. (2008). Development of protease inhibitors for protozoan infections. *Current opinion in infectious diseases*, *21*(6), 668-672.
15. Kubisch, R., Fröhlich, T., Arnold, G. J., Schreiner, L., von Schwarzenberg, K., Roidl, A., ... & Wagner, E. (2014). V-ATPase inhibition by archazolid leads to lysosomal dysfunction resulting in impaired cathepsin B activation in vivo. *International journal of cancer*, *134*(10), 2478-2488.
16. Ravish, I., & Raghav, N. (2014). Curcumin as inhibitor of mammalian cathepsin B, cathepsin H, acid phosphatase and alkaline phosphatase: a

correlation with pharmacological activities. *Medicinal Chemistry Research*, *23*, 2847-2855.

17. Ghosh, A., Banerjee, T., Bhandary, S., &Surolia, A. (2014). Formulation of nanotized curcumin and demonstration of its antimalarial efficacy. *International journal of nanomedicine*, 5373-5387.
18. Jamil, S. N. H., Ali, A. H., Feroz, S. R., Lam, S. D., Agustar, H. K., Mohd Abd Razak, M. R., & Latip, J. (2023). Curcumin and its derivatives as potential antimalarial and anti-inflammatory agents: a review on structure–activity relationship and mechanism of action. *Pharmaceuticals*, *16*(4), 609.
19. Obeid, M. A., Alsaadi, M., &Aljabali, A. A. (2023). Recent updates in curcumin delivery. *Journal of liposome research*, *33*(1), 53-64.
20. Nourbakhsh, M., Noori, S., Aminzade, Z., Bayanati, M., Alemi, M., &Zarghi, A. (2023). Attenuation of Inflammatory Responses in Breast and Ovarian Cancer Cells by a Novel Chalcone Derivative and Its Increased Potency by Curcumin. *Mediators of Inflammation*, *2023*.
21. Zhang, Y., Liu, C., Ju, H., Jia, R., Gao, S., Liu, X., ... & Zhan, P. (2023). Chalcones: Diverse biological activities and structure–activity relationships. In *Privileged Scaffolds in Drug Discovery* (pp. 21-39). Academic Press.
22. Gan, X., Wu, Y., Zhu, M., Liu, B., Kong, M., Xi, Z., ... & Wu, J. (2024). Design, synthesis, and evaluation of cyclic C7-bridged monocarbonyl curcumin analogs containing an o-methoxy phenyl group as potential agents against gastric cancer. *Journal of Enzyme Inhibition and Medicinal Chemistry*, *39*(1), 2314233.
23. Prlić, A., Bliven, S., Rose, P. W., Bluhm, W. F., Bizon, C., Godzik, A., & Bourne, P. E. (2010). Pre-calculated protein structure alignments at the RCSB PDB website. *Bioinformatics*, *26*(23), 2983-2985.
24. Sievers, F., & Higgins, D. G. (2014). Clustal Omega, accurate alignment of very large numbers of sequences. *Multiple sequence alignment methods*, 105-116.
25. Bertoldo, J. B., Chiaradia-Delatorre, L. D., Mascarello, A., Leal, P. C., Cordeiro, M. N. S., Nunes, R. J., ... & Terenzi, H. (2015). Synthetic compounds from an in house library as inhibitors of falcipain-2 from Plasmodium falciparum. *Journal of Enzyme Inhibition and Medicinal Chemistry*, *30*(2), 299-307.
26. Singh, R., Kumar, P., Sindhu, J., Devi, M., Kumar, A., Lal, S., & Singh, D. (2023). Parsing structural fragments of thiazolidin-4-one based α-amylase inhibitors: A combined approach employing in vitro colorimetric screening and GA-MLR based QSAR modelling supported by molecular docking, molecular dynamics simulation and ADMET studies. *Computers in Biology and Medicine*, *157*, 106776.
27. Gackowski, M., Madriwala, B., & Koba, M. (2023). In silico design, docking simulation, and ANN-QSAR model for predicting the anticoagulant activity of thiourea isosteviol compounds as FXa inhibitors. *Chemical Papers*, *77*(11), 7027-7044.
28. Eberhardt, J., Santos-Martins, D., Tillack, A. F., & Forli, S. (2021). AutoDock Vina

Journal of Chemical Health Risks

www.jchr.org

JCHR (2025) 15(5), 465-493 | ISSN:2251-6727

1.2. 0: New docking methods, expanded force field, and python bindings. *Journal of chemical information and modeling*, *61*(8), 3891-3898.

29. Balachandar, S., Sethuram, M., Muthuraja, P., Shanmugavadivu, T., & Dhandapani, M. (2016). Ligand based pharmacophoric modelling and docking of bioactive pyrazolium 3-nitrophthalate (P3NP) on Bacillus subtilis, Aspergillus fumigatus and Aspergillus niger—Computational and Hirshfeld surface analysis. *Journal of Photochemistry and Photobiology B: Biology*, *163*, 352-365.
30. Dhanavade, M. J., Parulekar, R. S., Kamble, S. A., & Sonawane, K. D. (2016). Molecular modeling approach to explore the role of cathepsin B from Hordeum vulgare in the degradation of Aβ peptides. *Molecular bioSystems*, *12*(1), 162-168.
31. Hao, Y., Purtha, W., Cortesio, C., Rui, H., Gu, Y., Chen, H., ... & Huang, X. (2018). Crystal structures of human procathepsin H. *PLoS One*, *13*(7), e0200374.
32. Adams-Cioaba, M. A., Krupa, J. C., Xu, C., Mort, J. S., & Min, J. (2011). Structural basis for the recognition and cleavage of histone H3 by cathepsin L. *Nature communications*, *2*(1), 197.
33. Rana, D., Kalamuddin, M., Sundriyal, S., Jaiswal, V., Sharma, G., Sarma, K. D., ... &Mahindroo, N. (2020). Identification of antimalarial leads with dual falcipain-2 and falcipain-3 inhibitory activity. *Bioorganic & Medicinal Chemistry*, *28*(1), 115155.
34. Sharma, K., & Raghav, N. (2021). In-silico Interaction studies of curcumin and structurally related commercial drug afatinib and bicalutamide with probable anticancer targets. *Chemistry & Biology Interface*, *11*(5).
35. Garg, S., & Raghav, N. (2016). 2, 5-Diaryloxadiazoles and their precursors as novel inhibitors of cathepsins B, H and L. *Bioorganic Chemistry*, *67*, 64-74.
36. Srivastava, R. (2021). Theoretical studies on the molecular properties, toxicity, and biological efficacy of 21 new chemical entities. *ACS omega*, *6*(38), 24891-24901.
37. Sadhana, S., Gupta, A. K., & Amita, V. (2013). Molecular properties and bioactivity score of the Aloe vera antioxidant compounds-in order to lead finding. *Research Journal of Pharmaceutical, Biological and Chemical Sciences*, *4*(2), 876-881.
38. Lin, J., Sahakian, D. C., De Morais, S. M., Xu, J. J., Polzer, R. J., & Winter, S. M. (2003). The role of absorption, distribution, metabolism, excretion and toxicity in drug discovery. *Current topics in medicinal chemistry*, *3*(10), 1125-1154.
39. Kar, S., & Leszczynski, J. (2020). Open access in silico tools to predict the ADMET profiling of drug candidates. *Expert opinion on drug discovery*, *15*(12), 1473-1487.
40. Bakchi, B., Krishna, A. D., Sreecharan, E., Ganesh, V. B. J., Niharika, M., Maharshi, S., ... & Shaik, A. B. (2022). An overview on applications of SwissADME web tool in the design and development of anticancer, antitubercular and antimicrobial agents: A medicinal chemist's perspective. *Journal of Molecular Structure*, *1259*, 132712.
41. Cheng, F., Li, W., Zhou, Y., Shen, J., Wu, Z., Liu, G., ... & Tang, Y. (2012).

admetSAR: a comprehensive source and free tool for assessment of chemical ADMET properties.

42. Eberhardt, J., Santos-Martins, D., Tillack, A. F., & Forli, S. (2021). AutoDock Vina 1.2. 0: New docking methods, expanded force field, and python bindings. *Journal of chemical information and modeling*, *61*(8), 3891-3898.
43. Balachandar, S., Sethuram, M., Muthuraja, P., Shanmugavadivu, T., & Dhandapani, M. (2016). Ligand based pharmacophoric modelling and docking of bioactive pyrazolium 3-nitrophthalate (P3NP) on Bacillus subtilis, Aspergillus fumigatus and Aspergillus niger—Computational and Hirshfeld surface analysis. *Journal of Photochemistry and Photobiology B: Biology*, *163*, 352-365.
44. Nandi, S. (2017). QSAR of Imidazo [1, 2-a] pyridine Ethers as Mycobacterial Adenosine Triphosphate Synthase Inhibitors against Tuberculosis. *EC Microbiology*, *8*, 280-293.
45. Bouarra, N., Kherouf, S., Nadji, N., Nouri, L., Boudjemaa, A., Djerad, S., &Bachari, K. (2024). Quantitative structure-electrochemistry relationship modeling of a series of anticancer agents using MLR and ANN approaches. *Chemical Product and Process Modeling*, *19*(2), 251-262.
46. Sharma, K., & Raghav, N. (2021). Curcumin analogs as anti-cathepsins agents: Designing, virtual screening, and molecular docking analysis. *Computational Toxicology*, *19*, 100174.
47. Laufkötter, O., Sturm, N., Bajorath, J., Chen, H., & Engkvist, O. (2019). Combining structural and bioactivity-based fingerprints improves prediction performance and scaffold hopping capability. *Journal of cheminformatics*, *11*, 1-14.
48. DiMasi, J. A. (2001). Risks in new drug development: approval success rates for investigational drugs. *Clinical Pharmacology & Therapeutics*, *69*(5), 297-307.